ESKİŞEHİR TECHNICAL UNIVERSITY JOURNAL OF SCIENCE AND TECHNOLOGY
A- APPLIED SCIENCES AND ENGINEERING

2018, 19(4), pp. 991 - 1000, DOI: 10.18038/aubtda.446535

FINITE ELEMENT ANALYSIS OF NANOINDENTATION ON NANOLAMINATED MATERIALS

Sezer ÖZERİNÇ [1,*]

[1] Mechanical Engineering Department, Faculty of Engineering, Middle East Technical University, Ankara, Turkey

ABSTRACT

Nanoindentation is a widely used tool for probing the mechanical properties of materials at the nanoscale. The analysis of the load-displacement curve obtained from nanoindentation provides the hardness and elastic modulus of the material. While hardness is a useful parameter for comparing different alloys and understanding tribological behavior, yield strength is a more useful parameter for alloy design and application in general. The yield strength of a nanoindentation-tested material can be estimated by combining the hardness result with the Tabor factor. This approach is well-established for homogeneous and isotropic materials; however, the application of the approach to recently developed laminated nanocomposites requires a better understanding of the plasticity under nanoindentation. Due to the complicated stress state and the nonhomogeneous geometry of the nanolaminated structure, there is a need to employ numerical methods for this analysis. In this study, the mechanical behavior of a model system of nanolaminated Cu-Nb under nanoindentation was investigated, through modeling the test using finite element method. The force-controlled simulation provided the load-displacement curve that would be obtained from an actual experiment, and Oliver-Pharr method was employed to obtain the hardness of the nanocomposite. The results show that the rule-of-mixture is a good approximation for estimating the nanoindentation hardness of the composites, if the mechanical properties of the constituents are known.

Keywords: Mechanical testing, nanoindentation, Finite element modeling, Nanostructured materials, Nanolaminated metals

1. INTRODUCTION

Nanoindentation is a commonly used technique for determining the hardness and elastic modulus of thin films and nanomaterials. In this technique, a nanoindenter indents the surface of the specimen with a diamond tip, and measures the force on the sample and the displacement into the surface of the sample. The load-displacement curve obtained is usually analyzed by the Oliver-Pharr method (1) to obtain the mechanical properties of the tested material.

Although nanoindentation measurements are quick and practical, the resulting hardness value is not as useful as the yield strength of a material from an engineering perspective. Although there is not a simple relationship between the yield strength and hardness of a material, Tabor factor is commonly used to obtain a first approximation. The Tabor factor is defined as:

$$C = \frac{H}{\sigma_y} \tag{1}$$

In this equation, C is Tabor factor, H is hardness, σ_y is yield strength (2). For a perfectly plastic material, Tabor factor varies in between 2.8 and 3.1 (3).

Conventional uniaxial mechanical testing is either very tedious or not possible for most thin films, coatings, and nanostructured materials. In these cases, the strength of the material can be estimated through nanoindentation with the use of Eq. (1). A limitation of this approach is that the Oliver-Pharr methodology and the theory behind the Tabor factor assume a homogeneous and isotropic material. On the other hand, many new generation coatings and nanostructures are not homogeneous, some

*Corresponding Author: ozerinc@metu.edu.tr
Received: 21.07.2018 Accepted: 19.11.2018

examples include superlattice coatings such as TiN/TiAlN (4) and high strength metallic nanolaminates such as Cu/Nb (5) (see Figure 1).

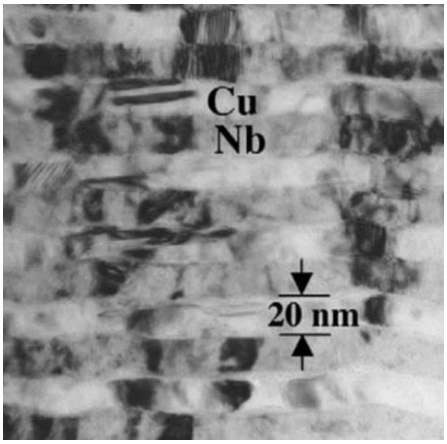

Figure 1. Transmission electron microscopy image of a Cu-Nb nanolaminate (5).

Nanolaminates are composites formed by alternating layers of two or more materials with different mechanical properties. Nanoindentation tests combined with Oliver-Pharr analyses are widely performed on them to understand their mechanical behavior (6). Although these materials are not homogeneous, hardness results are usually interpreted as an indication of the yield strength through Tabor factor. Since the nanoindentation measurement itself does not provide detailed knowledge of the deformation morphology, the direct application of Tabor factor is not completely justified. In addition, application of the rule of mixture to estimate the mechanical properties of nanolaminates is commonly employed as a first approximation (7). Similar to the direct application of Tabor factor, the rule-of-mixture approach also requires validation for the reliable analysis and interpretation of experimental measurements on nanolaminates. For more systematic and reliable characterization of nanolaminates and nanocomposites in general, there is a need to quantitatively relate their structural properties to their nanoindentation hardness. A better understanding of this relation will enable a more accurate interpretation of the mechanical testing of most nanomaterials.

For a nanolaminate, nanoindentation experiments can only provide information about the convoluted plastic response of the material, therefore it is not possible to measure the mechanical properties of the individual layers. In order to gain insight to the problem, there is a need to both know the strength of each layer of the composite, and the indentation hardness. Since this is not experimentally feasible, finite element modeling becomes and alternative and effective approach, in which the complicated stress state below the indenter is accurately computed upon the detailed definition of the layer mechanical properties.

There has been extensive work on the finite element modeling of nanoindentation (8). Most of the work focused on homogeneous materials, and usually aimed at understanding the effect of experimental artifacts such as surface roughness and substrate effects on the measurements (9). Previous work on nanoindentation modeling of laminated structures has been quite limited and mostly focused on hard coatings. Spherical indentation simulations performed on TiSiN/TiN hard coatings demonstrated that a multilayered structure can reduce the maximum shear stress under the indenter, which can delay crack formation and associated coating failure (10). Another study modeled the Berkovich indentation on Al/SiC metal/ceramic composites and showed that Al layers can undergo plastic deformation even during unloading, which renders the nanoindentation-based elastic modulus measurements difficult (11). Although these studies gave insight to the deformation behavior of nanolaminated materials under indentation, the effect of each layer's properties on the hardness response of nanolaminates remained unexplored. This work aims to fill this gap in the literature by

finite-element modeling the nanoindentation behavior of a nanolayered system and to obtain a relationship between the strength of their constituent structures and their hardness.

2. MATERIALS AND METHODS

Nanoindentation measurements were modeled by using finite element analysis through ABAQUS CAE 2016. Nanoindentation experiments commonly employ Berkovich tips in the form of a triangular pyramid. While this geometry ideally requires a 3D model, previous studies have shown that assuming a conical tip with an area function identical to that of the Berkovich tip yields similar results (12). Based on this finding, a 2D axisymmetric model was utilized. Figure 2 shows the model geometry. The specimen was a disc-shaped cylinder, corresponding to a rectangle in the axisymmetric model with dimensions of 10 μm thickness and 40 μm width. The indenter tip had a conical geometry, corresponding to a triangle with an included angle of 140.6° (13). The Berkovich tip was truncated at a height of 2 μm.

The first step was the verification of the approach for the case of a homogeneous and isotropic sample. Figure 2 shows the mesh used with this model that consists of a total of 25697 four-node elements. The mesh size decreased towards the tip of the diamond and towards the top side of the specimen that will experience the largest strain. For example, the characteristic element size was about 5 nm around the tip of the diamond whereas it became 500 nm next to the base of the diamond tip. This non-uniform mesh structure is a commonly utilized approach to improve the accuracy of the numerical solution in regions of high plastic activity while maintaining relatively short computational times.

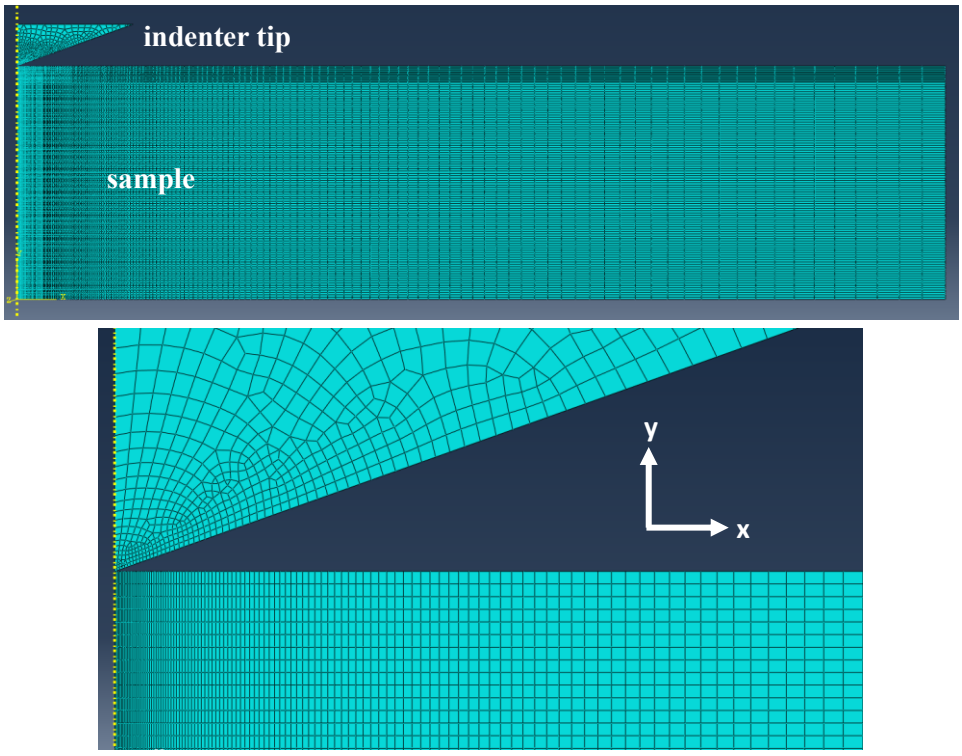

Figure 2. At the top, the axisymmetric model of the nanoindentation showing the details of the mesh, and at the bottom, a close-up view of the refined mesh around the contact point.

The base of the specimen was fixed while the motion along the symmetry axis was restricted to y-direction only. The top surface and the right-hand-side edge of the specimen was free to move. When it comes to the diamond tip, the motion along the symmetry axis was restricted to y-direction, similar

to the sample, and the right bottom side of the diamond tip was free. The simulation employed force control, and this control was achieved through a uniformly distributed load applied at the top side of the indenter. In actual experiments, the diamond tip, which is attached to the loading column of the nanoindenter, usually gets actuated by magnetic or electrostatic transducers at the top. Therefore, this distributed-force boundary condition gives an accurate representation of the actual experimental conditions. The friction between the diamond tip and the specimen was defined as 0.2, a value commonly used for nanoscale contacts (14). On the other hand, previous studies indicate that the friction coefficient does not dramatically alter the hardness results (8). The model considered diamond as a purely elastic material without any plasticity, and the samples were assumed linear elastic and perfectly plastic.

During the simulation, the indenter load linearly increased from 0 mN to 120 mN, followed by a linear unloading back to 0 mN. The motion of the diamond indenter towards the sample was recorded for every increment of loading throughout the simulation. As a result, a force on sample-displacement into surface plot was obtained, that is analogous to the output of an actual indentation experiment. Figure 3 shows an example force-displacement curve that was obtained from the simulation.

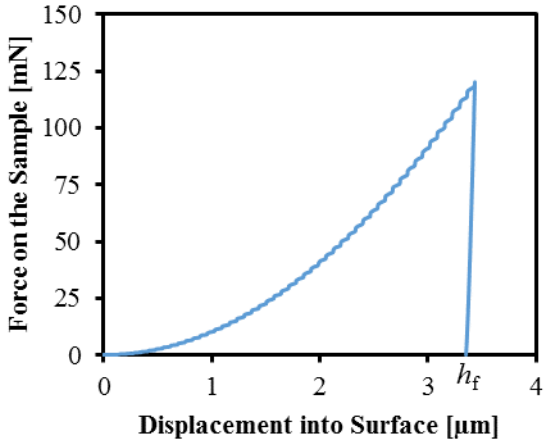

Figure 3. Force-displacement curve obtained from the indentation simulation performed.

3. RESULTS AND DISCUSSION

3.1. Analysis of a Homogeneous, Perfectly Plastic Material

Before simulating the indentation of the nanolaminate, the simulation results were verified by considering a perfectly plastic, homogeneous and isotropic sample. Table 1 summarizes the mechanical properties of this model material, given as an input to ABAQUS.

Table 1. The mechanical properties of the perfectly plastic sample for the verification simulation.

Elastic Modulus [GPa]	Yield Strength [MPa]	Poisson's Ratio
70	100	0.34

Nanoindentation hardness of a material is defined as:

$$H = \frac{P_{max}}{A_p} \tag{2}$$

where H is the hardness, P_{max} is the maximum load during indentation, and A_p is the projected contact area between the indenter tip and the sample at maximum load. The nanoindenter measures P_{max} directly, however it is not trivial to calculate the contact area, A_p. For the calculation of A_p the well-established Oliver-Pharr method was used (1). The full details of this method is available in the literature (1), and here the procedure is outlined. The first step in the method is the calculation of the contact stiffness, S, of the indent at the point of maximum load. For this purpose, a power-law curve fit was performed on the unloading segment of the force-displacement curve in the form:

$$P = A(h - h_f)^m \tag{3}$$

where, P is load as a function of h, which is the displacement into surface. h_f is the x-intercept of the unloading curve, as labeled in Figure 3. Then the contact stiffness corresponds to $S = dP / dh$ calculated at h_{max}, where h_{max} is the maximum displacement into sample. Once stiffness is found, the next step is the calculation of the contact depth, h_c. If one considers a three dimensional surface as the collection of points where the tip and the sample touches each other, the contact depth is the height of this surface along the sample surface normal (see Figure 7 for a graphical definition). Contact depth can be determined by utilizing Sneddon's expression (15):

$$h_c = h_{max} - \epsilon \frac{P_{max}}{S} \tag{4}$$

where for axisymmetric indenters, epsilon is defined as (15):

$$\epsilon = \frac{2}{\pi}(\pi - 2) \tag{5}$$

There is a direct relationship between the contact depth of the indenter and the projected area of the contact, defined by the geometry of the indenter itself. For our case, it is identical to that of a Berkovich tip, defined as:

$$A_p = 24.5 h_c^2 \tag{6}$$

The area A_p is the projected area in Equation (2), that was the missing information for the calculation of the hardness. By following this procedure, the hardness of the model material with a yield strength of 100 MPa, was calculated as 286 MPa. Using Eq. (1), this gives a Tabor factor of 2.86, which is in agreement of the previously mentioned range of Tabor factors (2.8–3.1). It should be noted that the exact Tabor factor can depend on many parameters such as the amount of pile-up, friction, and elastic properties of the material. Therefore, the close agreement between the theory and simulations observed here was considered as a verification of the modeling approach.

In order to further verify the validity and accuracy of the numerical approach, a previous study of nanoindentation on bulk Al by Knapp et al. was repeated (8). All the simulation parameters were set to be identical to this selected work. The material was modeled as an isotropic, elastic-plastic solid, by using the classical metal plasticity model employing von Mises yield criterion. The strain hardening of Al was taken into account by using the stress-strain data provided in the study (8), and friction coefficient was taken as 0.2. Figure 4 compares our findings with the results of Knapp et al. (8), and demonstrates the excellent agreement between the two independent work. This agreement was considered as a more complete verification of the model, enabling further studies on different systems.

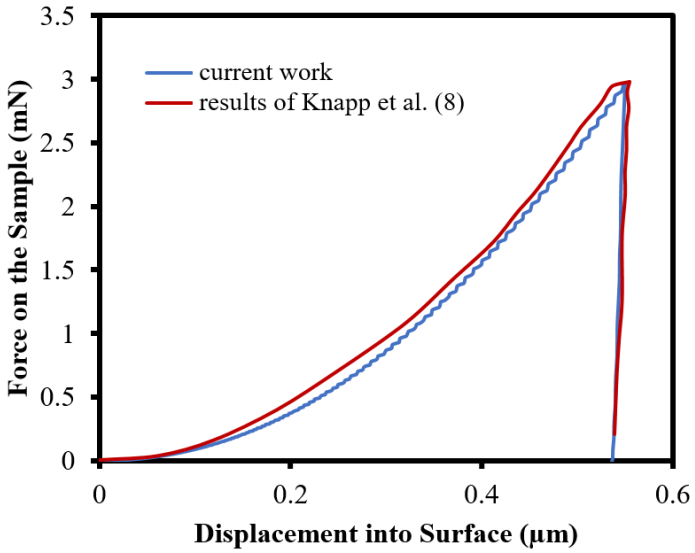

Figure 4. Force-displacement curves of nanoindentation on Al, comparing the results of the current work and results from literature (8).

3.2. Analysis of the Nanolaminated Composite

Upon the verification of the modeling for a homogeneous, perfectly plastic material, the indentation response of a widely studied nanostructured material, Cu/Nb nanolaminate, was investigated. Cu/Nb nanolaminates have recently become the subject of many experimental and theoretical studies due to its outstanding strength (16), thermal stability and radiation resistance (17), making it a promising new generation material for a wide range of applications.

Figure 5 shows a schematic view of the sample geometry and loading configuration. The model included a total of 100 alternating layers of Cu and Nb, with a layer thickness of 100 nm, a layer thickness that has been commonly produced and characterized in detail in the literature (5). For the mechanical properties of each layer, we used the strength of nanocrystalline Cu and Nb at an average grain size of 100 nm, by interpolating the available literature data (18,19). Assuming a grain size similar to layer thickness is a realistic approach, as the grain sizes of these structures and their layer thickness tend to be proportional to each other in practice. The properties used for each layer are summarized in Table 2.

Strain hardening is not pronounced in nanocrystalline materials (20), and as an approximation, we considered each layer as perfectly plastic. In experimental studies, nanolaminated metals are mostly produced by physical vapor deposition (5) and accumulative roll bonding (21). Both of these approaches provide clean and smooth interfaces with good adhesion between the layers. Based on this fact, we assumed perfect adhesion in between layers. Apart from the above-mentioned details, the analyses of the nanolaminated structure followed the same steps as those of the verification sample described in the previous section. The sample-indenter model, boundary conditions and the subsequent Oliver-Pharr analyses remained the same. A similar mesh density was used, and the only difference was the termination of the elements at the interfaces for consistent property mapping.

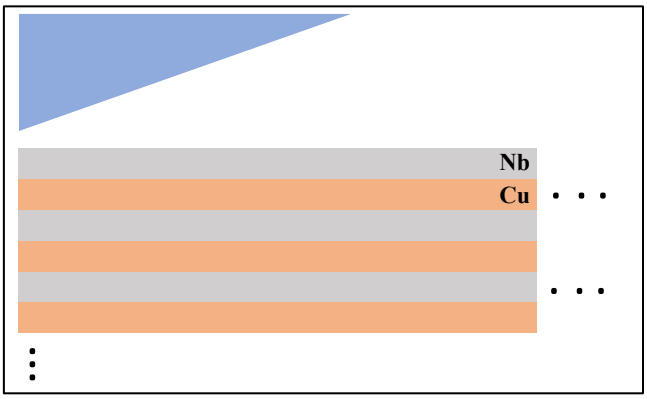

Figure 5. A schematic view of the sample and the loading geometry for nanolaminate indentation. The relative size of the indenter and the sample is not to scale.

Table 2. Mechanical properties of Cu and Nb layers used as an input to COMSOL (18, 19)

Material	Modulus of Elasticity [GPa]	Yield Strength [MPa]	Poisson's Ratio
Cu	117	370	0.34
Nb	105	900	0.40

The simulation and its analyses through Oliver-Pharr method provided a nanolaminate hardness of 1650 MPa. As an alternative path, we can use the rule-of-mixture and calculate the average yield strength and hardness of the composite. Since the layer thicknesses are identical for both Cu and Nb, rule-of-mixture becomes the arithmetic average:

$$\sigma_{predicted} = \frac{\sigma_{Cu} + \sigma_{Nb}}{2} \tag{7}$$

where $\sigma_{\text{predicted}}$ is the yield strength of the composite and σ_{Cu} and σ_{Nb} are the yield strengths of nanocrystalline Cu and Nb given as an input to the simulation. Then the hardness of the nanolaminate can be estimated by the use of Tabor factor:

$$H_{predicted} = C\frac{\sigma_{Cu} + \sigma_{Nb}}{2} \tag{7}$$

where we found C as 2.86 in the previous section. This results in a hardness of 1820 MPa which is close to that obtained by the finite element simulation (1650 MPa).

Table 3 summarizes the simulation results and gives a comparison between layer properties and the nanolaminate hardness. The results imply that the nanoindentation response of a composite can be estimated from the rule-of-mixture combined with Tabor factor as a first approximation.

Table 3. The yield strengths of Cu and Nb as inputs to the simulation, and the hardness predicted from rule of mixture and finite element analysis.

Material	Explanation	Yield Strength [MPa]	Hardness [MPa]
Cu	Input to the model	370	-
Nb	Input to the model	900	-
Cu-Nb nanolaminate	Rule of mixture prediction	635	1820*
Cu-Nb nanolaminate	Simulation result	577*	1650

*Hardness or yield strength calculated with Tabor factor, C = 2.86.

For a better interpretation of this result, first consider the compression testing of a cylindrical nanolaminated specimen, with loading direction being perpendicular to the layers, as demonstrated in

Figure 6. In such a loading geometry, the softer layer will plastically deform first, therefore, the yield strength of the material will tend to resemble that of the softer layer, while the harder layer will start affecting the results upon sufficient strain hardening of the softer layer. At first glance, one would expect a similar behavior for nanoindentation, where the softer layer would dominate the plastic response. However, since nanoindentation results in an average plastic strain of about 8% below the indenter (22), a high level of deformation plays a role in the force-displacement response. Even if the material is perfectly plastic, this 8% deformation requires extensive thinning of the softer layer, which requires the flow of the squeezed layer radially outward. Since the layers are very thin when compared to the indentation depth, such a flow results in a very high hydrostatic stress, and this higher stress will start plastically deforming the harder layers. As a result, the hardness of the nanolaminate is not close to that of the softer layer; instead, it is approximately equal to the rule-of-mixture value that suggests co-deformation of the layers at the same time.

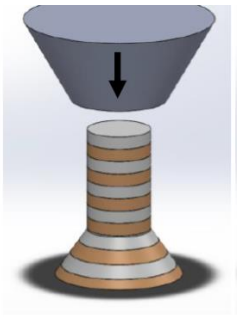

Figure 6. A schematic description of the compression experiment on a nanolaminate.

Figure 7 demonstrates a verification of this reasoning by taking a closer look at the deformation path of the nanolayers. The contrast provided by the stress intensity shows the deformation morphology of individual layers, where a higher stress is present in Nb layers (blue color). The layers just under the indenter tip goes through considerable strain, and it can be seen that there is no obvious difference between the thinning of the Cu and Nb layers. This demonstrates that the layers co-deform, and the plastic response is a average of the response of the Cu and Nb layers. Nevertheless, it should be noted that Nb tends to experience higher stress levels, indicating that Cu starts deforming at the onset of plasticity. However, as plasticity continues, Nb participates in deformation and an averaged response is observed.

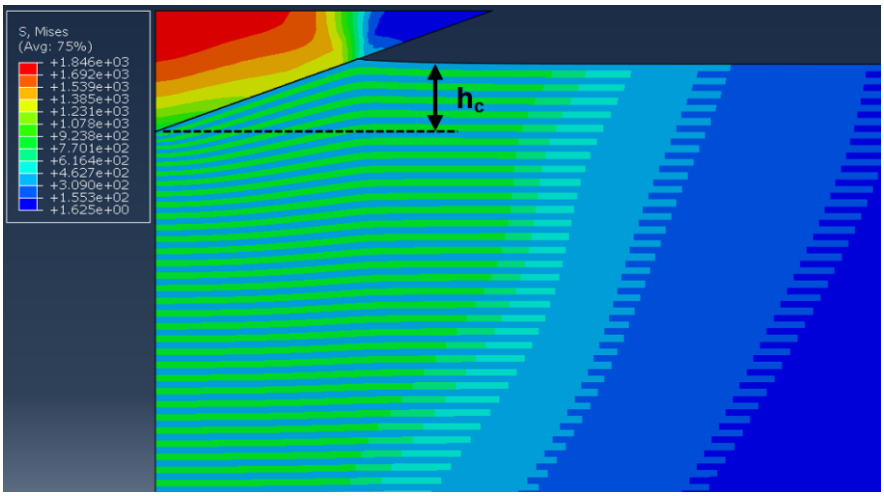

Figure 7. The von Mises stress state of the diamond indenter and the nanolayers during indentation at the maximum load. Definition of contact depth is presented to facilitate the discussion in Section 3.1.

Another interesting observation is the fact that the stress levels below the indenter continues to be high for depths many times that of the indentation depth. This is in agreement with the experimental and numerical findings that plasticity under the indenter can extend up to ten times the indentation depth (23).

4. CONCLUSIONS

This work analyzed the nanoindentation response of metallic nanolaminates by utilizing finite element modeling. The results show that the nanolaminate hardness can be estimated by the rule-of-mixture approach if the hardness of the individual layers are known. This suggests that nanolaminates with layers of very different mechanical properties co-deform under indentation. A close observation of the deformation morphology of the nanolaminates further support this argument.

From a practical point of view, hardness of confined layers is difficult to predict, therefore the results cannot be directly used for the estimation of the strength. On the other hand, the demonstrated co-deformation behavior and the finding of the validity of the rule-of-mixture is very valuable and will enable the better interpretation of experimental results on the mechanical properties of nanolaminates and other nanocomposite materials.

ACKNOWLEDGEMENTS

This research was supported by TÜBİTAK 3501 CAREER Award under Project No. 116M429 and by TÜBİTAK 2232 Research Fellowship under project No. 117C001.

REFERENCES

[1] Oliver WC, Pharr GM. An improved technique for determining hardness and elastic modulus using load and displacement sensing indentation experiments. J Mater Res 1992; 7: 1564–1583.

[2] Tabor D. The Hardness of Metals. Oxford, United Kingdom: Oxford University Press, 2000.

[3] Tirupataiah Y, Sundararajan G. On the constraint factor associated with the indentation of work-hardening materials with a spherical ball. Mater Transac A 1991; 22: 2375–2384.

[4] Hahn R, Bartosik M, Soler R, Kirchlechner C, Dehm G, Mayrhofer PH. Superlattice effect for enhanced fracture toughness of hard coatings. Scripta Mater 2016; 124: 67–70.

[5] Misra A, Hirth JP, Hoagland RG. Length-scale-dependent deformation mechanisms in incoherent metallic multilayered composites. Acta Mater 2005; 53: 4817–4824.

[6] Wang J, Zhou Q, Shao S, Misra A. Strength and plasticity of nanolaminated materials. Mater Res Lett 2017; 5: 1–19.

[7] Vella JB, Mann AB, Kung H, Chien CL, Weihs TP, Cammarata RC. Mechanical properties of nanostructured amorphous metal multilayer thin films. J Mater Res 2004; 19: 1840–1848.

[8] Knapp JA, Follstaedt DM, Myers SM, Barbour JC, Friedmann TA. Finite-element modeling of nanoindentation. J Appl Phys 1999; 85: 1460–1474.

[9] Xu ZH, Rowcliffe D. Finite element analysis of substrate effects on indentation behaviour of thin films. Thin Solid Films 2004; 447–448: 399–405.

[10] Zhao X, Xie Z, Munroe P. Nanoindentation of hard multilayer coatings: Finite element modelling. Mater Sci Eng A 2011; 528: 1111–1116.

[11] Tang G, Singh DRP, Shen YL, Chawla N. Elastic properties of metal–ceramic nanolaminates measured by nanoindentation. Mater Sci Eng A 2009; 502: 79–84.

[12] Lichinchi M, Lenardi C, Haupt J, Vitali R. Simulation of Berkovich nanoindentation experiments on thin films using finite element method. Thin Solid Films 1998; 312: 240–248.

[13] Wang Y. Effects of indenter angle and friction on the mechanical properties of film materials. Results Phys 2016; 6: 509–514.

[14] Huang X, Pelegri AA. Finite element analysis on nanoindentation with friction contact at the film/substrate interface. Compos Sci and Technol 2007; 67: 1311–1319.

[15] Sneddon IN. The relation between load and penetration in the axisymmetric boussinesq problem for a punch of arbitrary profile. Int J Eng Sci 1965; 3: 47–57.

[16] Mara NA, Bhattacharyya D, Dickerson P, Hoagland RG, Misra A. Deformability of ultrahigh strength 5nm Cu/Nb nanolayered composites. Appl Phys Lett 2008; 92: 231901.

[17] Demkowicz MJ, Hoagland RG, Hirth JP. Interface Structure and Radiation Damage Resistance in Cu-Nb Multilayer Nanocomposites. Phys Rev Lett 2008; 100: 136102.

[18] Özerinç S, Tai K, Vo NQ, Bellon P, Averback RS, King WP. Grain boundary doping strengthens nanocrystalline copper alloys. Scripta Mater 2012; 67: 720–723.

[19] Popova EN, Popov VV, Romanov EP, Pilyugin VP. Effect of the degree of deformation on the structure and thermal stability of nanocrystalline niobium produced by high-pressure torsion. Phys Met Metallogr 2007; 103: 407–413.

[20] Huang H, Spaepen F. Tensile testing of free-standing Cu, Ag and Al thin films and Ag/Cu multilayers. Acta Mater 2000; 48: 3261–3269.

[21] Beyerlein IJ, Mara NA, Carpenter JS, Nizolek T, Mook WM, Wynn TA, McCabe RJ, Mayeur JR, Kang K, Zhen S, et al. Interface-driven microstructure development and ultra high strength of bulk nanostructured Cu-Nb multilayers fabricated by severe plastic deformation. J Mater Res 2013; 28: 1799–1812.

[22] Bahr DF, Kramer DE, Gerberich WW. Non-linear deformation mechanisms during nanoindentation. Acta Mater 1998; 46: 3605–3617.

[23] D. Nix W. Elastic and plastic properties of thin films on substrates: nanoindentation techniques. Mater Sci Eng A 1997; 234–236: 37–44.